Pattern Recognition Letters 38 (2014) 20–25

Contents lists available at ScienceDirect

Pattern Recognition Letters

journal homepage: www.elsevier.com/locate/patrec

Focusing in thermal imagery using morphological gradient operator

Myung Geun Chun [a,*], Seong G. Kong [b]

[a] Department of Electronics Engineering, Chungbuk National University, Cheongju, Chungbuk 361-763, South Korea
[b] Imaging and Pattern Recognition Laboratory, Department of Electrical and Computer Engineering, Temple University, Philadelphia, PA 19122, USA

ARTICLE INFO

Article history:
Received 6 March 2013
Available online 31 October 2013

Communicated by Nappi Michele

Keywords:
Morphological gradient
Thermal imagery
Focus
Face recognition
Focus measure

ABSTRACT

This paper presents focusing on an object of interest in thermal infrared (IR) imagery using the morphological gradient operator. Most existing focus metrics measure the degree of sharpness on the edge of an object in the field of view, often based on the local gradient operators of pixel brightness intensity. However, such focus measures may fail to find the optimal focusing distance to the object in thermal IR images, where strong edge components of an object do not exist. In particular, when the end goal of image acquisition is object recognition, focusing on an object must retain prominent features of the object for recognition. In this paper, the performances of various focus measures are evaluated in terms of sharpness as well as recognition accuracies for face recognition in thermal IR images. Experiment results show that the morphological gradient operator outperforms conventional gradient operators in terms of autofocusing resolution metric as well as face recognition accuracy.

1. Introduction

In an image acquisition process, an object of interest within the field of view of a camera must be well-focused to obtain its full details for visual evaluation or computerized processing. An optical camera can be focused on an object in the scene at a lens position that gives the sharpest image of the object formed on the image plane. The distance from the lens to the principal focus is called the focal length, where the lights from a point on the object converge. A focus measure finds the sharpness of an image at different lens positions. When the end goal of image acquisition is object recognition, a focused object of interest in a scene must retain the visual features that are critical in object recognition. Most existing focus measures, however, compute the degree of sharpness on the edge of an object, rather than the features of the object. Therefore a focus measure that delivers an in-focus image of an object must preserve the details for object recognition as well as for visual evaluation.

Thermal infrared (IR) spectrum comprising mid-wave IR (MWIR) in the spectral range of 3–5 μm and long-wave IR (LWIR) of 8–14 μm has been suggested as an alternative source of information for object recognition. Thermal IR imaging sensors measure the heat energy radiated, not reflected, from the object. IR energy can be viewed in any light conditions and is less subject to scattering and absorption by smoke or dust than the visible light. Face recognition using different imaging modalities, particularly IR imaging sensors, has become an area of growing interest (Kong et al., 2005; Chen et al., 2005). The use of thermal IR imagery has demonstrated performance improvements of face recognition in uncontrolled illumination conditions, including low illumination or even in darkness.

Focusing on a face object in a thermal scene is often challenging due to a significant amount of diffraction blur in thermal imaging since the refractive index decreases as the wavelength increases. In thermal IR imaging, it is challenging to visually find an in-focus object in the scene due to lack of strong edge components. In visible imaging, chromatic distortion caused by the defocusing problem can be easily dealt since the wavelength is relatively short. The defocusing problem in thermal imaging of longer wavelength can be 5–10 times more significant than in the visible imaging. Therefore, it is important to develop robust and objective criteria to evaluate whether a given thermal IR image is in-focus. It is relatively recent to study focusing in thermal IR imagery than in the visible spectrum (Pertuz et al., 2013). Various focus measures in thermal IR imaging were discussed in Faundez-Zanuy et al. (2011) along with a thermographic image database, suitable for the analysis of automatic focusing measures. Among their 10 different databases, a thermal face image database consisting of a set of human facial images was used to test autofocusing. However, there were no quantitative comparisons among the five existing focus measures. Since they manually selected in-focus (optimal) thermal face images, a proper evaluation of focus measures in terms of face recognition was not performed. Face recognition performance can be significantly influenced by the image quality (Sang et al., 2009). According to International Standard ISO/IEC 29794-5, out-of-focus,

* Corresponding author. Tel.: +82 43 261 2388.
E-mail addresses: mgchun@chungbuk.ac.kr (M.G. Chun), skong@temple.edu (S.G. Kong).

0167-8655/$ - see front matter Crown Copyright © 2013 Published by Elsevier B.V. All rights reserved.
http://dx.doi.org/10.1016/j.patrec.2013.10.023

non-frontal posture and side lighting are regarded as primary elements responsible for poor face image quality.

This paper investigates the performances of various local gradient operators on focusing in thermal imagery for qualitative as well as quantitative analysis including face recognition accuracy. We evaluate and compare several existing focus measures with a new focus measure using the morphological gradient operator in thermal imaging. Thermal imagery often shows a narrow dynamic range in gray level intensity with small bright and dark artifacts. Therefore, we adopt the morphological gradient operator which highlights the gray-level transition and reduces small bright and dark artifacts. Morphological dilation operation locally brightens the image according to the geometry of structuring element, while the erosion can locally darken the image. The morphological gradient operator, which finds the difference between the dilated image and eroded image, highlights the gray-level transition. With a proper selection of the threshold value, the dilation and erosion process removes small bright and dark artifacts. Autofocus resolution metric (ARM) has been used to quantify the shape of the focus measure curve (Xie et al., 2006). We used the Faundez-Zanuy database to evaluate the usefulness of five popular focus measures for the purpose of determining the optimal focus position. Experiment results on face recognition in thermal IR imaging show that the focus measure with the morphological gradient operator outperforms other focus metrics including the popular focus measures investigated in Faundez-Zanuy et al. (2011) in terms of low ARM, monotonicity, and the zero offset properties.

2. Focus measures and performance metrics

2.1. Existing focus measures

A number of focus measures have been investigated in the acquisition of various types of images including microscopic images and thermal IR images. A desirable focus measure is expected to satisfy some of common requirements (Faundez-Zanuy et al., 2011; Huang and Jing, 2007):

- unimodal distribution of focusing performance with a unique maximum at the in-focus position;
- monotonicity of focusing performance outside the in-focus position;
- a steep slope with respect to the degree of blurring;
- minimal computational complexity.

In addition to such requirements, the following requirements are considered for focusing on the face in thermal images:

- consistent focusing position in enrollment and verification processes;
- a maximum focus value at the position resulting highest recognition accuracy.

Faundez-Zanuy et al. (2011) evaluated five focus measures to compare their focusing performances with thermal IR images: Energy of Image Gradient, Tenengrad, Energy of Laplacian, Sum-modified Laplacian, and the measure proposed by Crete et al. (2007). Energy of image gradient (EOG) finds the sum of squared directional gradients

$$\mathrm{EOG} = \sum_{x=1}^{M-1}\sum_{y=1}^{N-1}\left[I_x(x,y)^2 + I_y(x,y)^2\right] \tag{1}$$

where $I_x(x,y) = I(x+1,y) - I(x,y)$ and $I_y(x,y) = I(x,y+1) - I(x,y)$.

Tenengrad computes the sum of squared Sobel gradient magnitudes that exceed a discrimination threshold T:

$$\mathrm{Tenengrad} = \sum_{x=2}^{M-1}\sum_{y=2}^{N-1}\left[I_x(x,y)^2 + I_y(x,y)^2\right], \sqrt{I_x(x,y)^2 + I_y(x,y)^2} > T \tag{2}$$

where the gradient magnitude value is given by the Sobel operators such as

$$\begin{aligned} I_x(x,y) = &-I(x-1,y-1) - 2I(x-1,y) - I(x-1,y+1) \\ &+ I(x+1,y-1) + 2I(x+1,y) + I(x+1,y+1) \end{aligned} \tag{3}$$

$$\begin{aligned} I_y(x,y) = &-I(x-1,y-1) - 2I(x,y-1) - I(x+1,y-1) \\ &+ I(x-1,y+1) + 2I(x,y+1) + I(x+1,y+1) \end{aligned} \tag{4}$$

Energy of Laplacian (EOL) of an image is defined based on the second derivatives such as

$$\mathrm{EOL} = \sum_{x=2}^{M-1}\sum_{y=2}^{N-1}\left(\nabla_x^2 I(x,y) + \nabla_y^2 I(x,y)\right)^2 \tag{5}$$

where

$$\begin{aligned} \nabla_x^2 I(x,y) + \nabla_y^2 I(x,y) = &I(x+1,y) + I(x-1,y) + I(x,y+1) \\ &+ I(x,y-1) - 4I(x,y) \end{aligned} \tag{6}$$

Sum-modified Laplacian (SML) was proposed from the observation that the Laplacian second derivatives in the x and y directions can have opposite signs canceling each other.

$$\mathrm{SML} = \sum_{x=2}^{M-1}\sum_{y=2}^{N-1}\nabla_{ML}^2 I(x,y) \text{ for } \nabla_{ML}^2 I(x,y) > T \tag{7}$$

where

$$\begin{aligned} \nabla_{ML}^2 I(x,y) = &|2I(x,y) - I(x-1,y) - I(x+1,y)| \\ &+ |2I(x,y) - I(x,y-1) - I(x,y+1)| \end{aligned} \tag{8}$$

Crete et al. (2007) proposed a focus measure, based on the discrimination between different levels of blur perceptible in the image rather than transient characteristics in the same image. This measure calculates the degree of blurring, so the sharpness can be obtained as

$$\mathrm{Crete} = 1 - \max(Bi_v, Bi_h) \tag{9}$$

where Bi_v and Bi_h denote vertical and horizontal blur values that range from 0 to 1.

In addition to those five focus measures mentioned above, we also tested other popular focus measures for focusing in thermal imagery: Normalized variance, Cross sum-modified Laplacian, Histogram-based Entropy, and Steerable Filters-based measure. The variance represents the variations in gray level of image pixels. The normalized variance (NVAR) measure refers to the variance divided by the average μ (Santos et al., 1997):

$$\mathrm{NVAR} = \frac{1}{\mu MN}\sum_{x=1}^{M}\sum_{y=1}^{N}[I(x,y) - \mu]^2 \tag{10}$$

Cross sum-modified Laplacian (XSML) extends the sum of modified Laplacian with the diagonal terms (Thelen et al., 2009):

$$\mathrm{XSML} = \sum_{x=2}^{M-1}\sum_{y=1}^{N-1}\nabla_{XSML}^2 I(x,y) \tag{11}$$

where

$$\nabla^2_{XSML} I(x,y) = |2I(x,y) - I(x-1,y) - I(x+1,y)| + |2I(x,y) - I(x,y-1) - I(x,y+1)| + \frac{1}{\sqrt{2}}|2I(x,y) - I(x+1,y+1) - I(x-1,y-1)| + \frac{1}{\sqrt{2}}|2I(x,y) - I(x-1,y+1) - I(x+1,y-1)| \quad (12)$$

The histogram based entropy (HISE) has been used as a focus measure (Guo et al., 2008), where $p(i)$ denotes normalized frequency of gray level i. A focused image tends to have more gray levels than out-of-focus images.

$$\text{HISE} = -\sum_i p(i)\log_2 p(i) \quad (13)$$

The steerable filters-based (SFIL) measure (Minhas et al., 2012) is defined as the sum of filtered versions of an image with the derivatives Γ_x and Γ_y of a Gaussian filter in x- and y-directions:

$$\text{SFIL} = \sum_x \sum_y I_f(x,y) \quad (14)$$

where the filtered version $I_f(x,y)$ of image $I(x,y)$ is defined as

$$I_f(x,y) = \max_{i=1,\cdots,N} \{(\cos\theta_i)(I^* \Gamma_x) + (\sin\theta_i)(I^* \Gamma_y)\} \quad (15)$$

2.2. Performance metrics of a focus measure for face recognition in thermal images

Object recognition accuracy has been used as a metric to evaluate the performance of a focus measure in addition to sharpness when the end goal of image acquisition is object recognition. Face recognition addresses the problem of verifying or identifying a given person in the scene by comparing an input face image with the images stored in the database. A well-focused face object must retain the facial features that are useful in the recognition task. When one uses a focus measure for face recognition, a focused face image should provide the highest recognition accuracy. Also, a good focus measure must provide a high gradient in the focusing performance curve as well as a unimodal characteristic around the peak of sharpness.

This paper evaluates the performance of focus measures in terms of face recognition accuracy as well as sharpness. We check whether a focus measure reaches the maximum focusing performance value at the highest recognition accuracy position. Without loss of generality, we selected the principal component analysis (PCA) and linear discriminant analysis (LDA) as a face recognition engine to test the focus measures in object recognition. Let an $n \times n$ image x_i be represented by an $n^2 \times 1$ vector z_i. For a set of N face images $\mathrm{Z} = \{\mathrm{z}_1, \mathrm{z}_2, \ldots, \mathrm{z}_N\}$, the covariance matrix is defined as

$$C = \frac{1}{N}\sum_{i=1}^{N} (zi - \bar{z})(z_i - \bar{z})^T \quad (16)$$

$$\bar{z} = \frac{1}{N}\sum_{i=1}^{N} z_i \quad (17)$$

Let $E = \{\mathrm{e}_1, \mathrm{e}_2, \ldots, \mathrm{e}_r\}$ contain the r eigenvectors corresponding to r largest eigenvalues. An original image is now represented by projecting Z into the PCA-transformed space

$$X_i = \mathrm{E}^T(z_i - \bar{z}) \quad (18)$$

To perform classification of a new thermal face image z' using the PCA, we compute a Euclidean distance between a given image z' and z in the training set Z:

$$d(z,z') = ||g(z) - g(z')|| \quad (19)$$

where $g(z)$ and $g(z')$ are PCA transformed vector of thermal face image z and z′, respectively.

In LDA, we define the between-class scatter matrix S_B and the within-class scatter matrix S_W as

$$S_B = \sum_{i=1}^{c} N_i(\bar{z}_i - \bar{z})(\bar{z}_i - \bar{z})^T \quad (20)$$

$$S_W = \sum_{i=1}^{c} \sum_{z_k \in Z_i} (z_k - \bar{z}_i)(z_k - \bar{z}_i)^T \quad (21)$$

where $\bar{z}_i$ denotes the mean of class Z_i, $\bar{z}$ is given in (17), and N_i denotes the number of images in class Z_i. We find the optimal projection W_{opt} f the LDA as the matrix with orthogonal columns that maximize the ratio of the determinant of S_B to the determinant of S_W of the projected images,

$$W_{opt} = \arg\max_w \frac{|W^T S_B W|}{|W^T S_W W|} = [\mathrm{w}_1 \mathrm{w}_2 \cdots \mathrm{w}_m] \quad (22)$$

Where $\{\mathrm{w}_i | i = 1,2\cdots m\}$ denotes the set of generalized eigenvectors of S_B and S_W corresponding to m largest generalized eigenvalues. For more details on the implementation of the PCA and LDA, see (Belhumeur et al., 1997).

Monotonicity is checked using the normalized focus measure graph. Steepness with respect to the degree of blurring is also important since it indicates whether a focus measure can easily detect the in-focus position. For the purpose of comparison, all focusing performance curves are normalized. We assume that the focus measures are calculated at several discrete positions with a center at the in-focus position. Let p_0 be the in-focus position and $M(p)$ denote the focusing performance measure at the position p. Then the ARM is defined as:

$$\text{ARM} = \frac{1}{||M||_2}\left[\sum_p (p - p_0)^2 M^2(p)\right]^{1/2} \quad (23)$$

This definition is derived from the resolution used in Heidelberg uncertainty principle (Subbarao and Tyan, 1998). Lower value of the ARM provides higher resolution of the focused image. Computational complexities of various focus measures are compared in terms of execution time in Section 4.2.

3. Focusing on the face in a thermal image using the morphological gradient operator

The morphological gradient (MOGR) operator finds the pixels with sharp transitions in gray level in the image. In comparison with conventional gradient operators, morphological gradients are obtained from symmetrical structuring element that tends to depend less on edge directionality. The MOGR operator uses nonlinear operators such as ‘max’ and ‘min’ for dilation and erosion operations, respectively. The effect of performing erosion with positive structuring elements on a gray-scale image is that the bright artifacts in the input image are reduced. Similarly, the general effect of performing dilation on a gray-scale image is that dark artifacts either are reduced or eliminated. Since thermal face images usually contain a lot of bright and dark artifacts, so one can reduce the freckles using the morphological operations such as dilation and erosion. From the property of the difference between dilated and eroded images, morphological gradient can enhance the gray-level transitions in the image.

There are two ways to define the gray-scale dilation and erosion operators to select a structuring element among non-flat and flat ones (Gonzalez and Woods, 2010). Flat structuring elements are

widely used in practice. We adopt the symmetrical, flat structuring elements of unit value. Then gray-scale dilation $I \oplus b$ of image I by a structuring element b is defined as

$$(I \oplus b)(x,y) = \max_{(s,t)\in b}\{I(x-s,y-t)\} \tag{24}$$

Similarly, gray-scale erosion $I\Theta b$ is defined as

$$(I\Theta b)(x,y) = \min_{(s,t)\in b}\{I(x+s,y+t)\} \tag{25}$$

Then a morphological gradient $g(x,y)$ of an image I is given by the difference of the two

$$g(x,y) = (I \oplus b)(x,y) - (I\Theta b)(x,y) \tag{26}$$

The morphological gradient is defined as

$$\text{MOGR} = \sum_{x=1}^{M}\sum_{y=1}^{N} g^2(x,y) \quad \text{for} \quad g(x,y) \geq T \tag{27}$$

Fig. 1 visually compares edge detection performances of the MOGR operator and the Sobel operator on a face in a thermal IR image. The MOGR operator with a 3×3 structuring element and threshold $T = 20$ successfully finds the edges of facial features regardless of the orientation of the features. Though the gray level difference is not usually big in thermal imaging, the morphological gradient enhances the details of facial features with a small amount of bright and dark artifacts.

4. Experiment results

4.1. Thermal face image database and recognition

We captured 700 thermal IR images to measure temperature profile of human face from 10 individuals of various ethnicities including six Asians, two Caucasians, one African, and one Indian subjects. The imaging sensor used was a LWIR camera (FLIR, ThermoVision A40 M) with the spectral range from 7.5 to 13 μm. The temperature sensitivity of this camera is 0.08 °C at 30 °C and the spatial resolution (IFOV) is 1.3 mrad. For each subject, 70 images were taken at various poses and focal distances, i.e., 10 different poses at 7 focusing steps. The camera is equipped with motorized zoom with a maximum focal distance of 3.4 mm and each button press changes the focal distance by a unit focusing step of 0.1 mm.

For each of face images captured by the thermal IR camera of size 320×240, a face region is cropped into a subimage of size 112×92, which is the same image size as that of face images in the popular Olivetti Research Laboratory (ORL) database (Abate et al., 2007). The Temple University Thermal Face (TUTF) database consists of such 700 thermal IR images of the cropped face of size 112×92 of 10 subjects. Fig. 2 shows a few cropped face image samples in the TUTF database captured at different focusing steps. Due to the lack of visual features in thermal IR images, it is challenging to determine the in-focus position by visual evaluation.

We selected a face recognition engine based on either the PCA or the LDA for a training data set of 50 images corresponding to 5 poses selected randomly from 10 poses for each of 10 subjects at each focusing step. The remaining 50 images were used for testing. We selected 40 eigenvectors corresponding to 40 dominant eigenvalues to build the PCA classifier and used four discriminant vectors for LDA (Belhumeur et al., 1997). We performed face recognition on the thermal IR face image database and the recognition accuracy was used as a measure to find the ground-truth in-focus position. Table 1 summarizes face recognition rate and equal error rate for the images from the TUTF database at different focusing steps. The ground-truth in-focus position was chosen as the position where the highest recognition accuracy was obtained. The in-focus images produced the lowest equal error rate on average as well.

Focusing performance affects face recognition accuracies. Fig. 3 shows Receiver Operating Characteristics (ROC) of face recognition of in-focus (0) and out-of-focus (−1 and +1) images. When in-focus images were used for recognition, the PCA and LDA face recognition rates were as high as 98% with the EERs of 5.3% and 1.8%, respectively. The false acceptance rate (FAR) and false rejection rate (FRR) increased and so did the EER as the focus position shifted

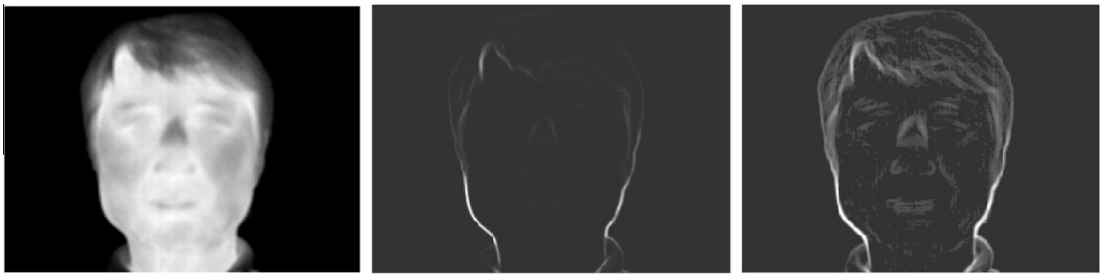

(a) (b) (c)

Fig. 1. Edge detection performance of the morphological gradient operator: (a) Original thermal IR face image; (b) Edge detection with the Sobel operator and (c) Edge detection with the MOGR operator.

(a) -2 (b) -1 (c) 0 (in-focus) (d) +1 (e) +2

Fig. 2. Sample thermal face images captured at five different focusing steps.

Table 1
Face recognition accuracy at different focus positions.

Performance		Focus position						
		−4	−3	−2	−1	0 (in-focus)	+1	+2
PCA	Recognition Rate (%)	92	96	96	92	98	94	84
	Equal Error Rate (%)	9.6	8.9	9.3	12.1	5.3	8.2	15.9
LDA	Recognition Rate (%)	90	94	92	92	98	98	96
	Equal Error Rate (%)	6.2	5.3	6.2	6.2	1.8	4.1	2.9

from in-focus to out-of-focus positions. When out-of-focus (+1) images were used for the PCA classifier, the face recognition rate dropped to 94% and the EER increased to 8.2%. On the other hand, when out-of-focus (+1) images were used for the LDA classifier, the face recognition rate remained the same as 98%, but the EER increased to 4.1%. LDA showed lower EERs and the same high recognition accuracy as the PCA at in-focus position.

4.2. Focusing experiment results

Faundez-Zanuy et al. (2011) studied various focus measures for focusing the objects in thermal images including human faces. Their database consists of a set of thermal face images acquired at different focus positions. The camera position was manually changed in 1 mm steps on a linear translation stage, up to a total of 96 positions. They investigated five popular focus measures for the focusing performances of individual focus measures with thermal images. It has been reported that the focus measure based on the Tenengrad operator failed to provide correct focus position by saying "We have observed that Tenengrad operator was unable to provide an accurate peak in some image sets..." In contrary to the observations, we found that the Tenengrad focus measure actually performed well for thermal images. The contradictory result came from the fact that they used a wrong Tenengrad operator formula with a missing minus sign described in Eq. (8) of Huang and Jing, 2007. We first tested the five focus measures using the thermal face database from Faundez-Zanuy et al. (2011) with a correct formulation of the Tenengrad focus measure. Fig. 4(a) shows the performance of the five focus measures applied to a set of 96 thermal face images taken at each focusing step. The zero focusing point shows the ground-truth in-focus step. The Tenengrad operator also shows reasonably good focusing results. Fig. 4(b) shows the focusing performances of the other four focus measures and the proposed MOGR focus measure. As mentioned in (Huang and Jing, 2007), desirable focus measures are required to show a large variation in focus measure value for different focusing positions. In Fig. 4(b), the MOGR operator shows a peak focus measure value at in-focus position while the focus measure decreases quickly as the focus position moves from in-focus position to out-of-positions. When we compared the focusing performances of all ten focus metrics in terms of the ARM, the MOGR operator showed the smallest ARM of 9.02 steps and the Tenengrad operator showed the second smallest value of 12.40 steps.

We repeated the same experiment to the 100 images at each focusing position in the TUTF database. Fig. 5 shows the average normalized focus measures at each focus position. Fig. 5(a) compares the average normalized focus measures of the five focus measures, EOG, Tenengrad, EOL, SML, and Crete. Fig. 5(b) shows the comparison results of the other five focus measures, NVAR, XSML, HISE, SFIL, and MOGR. Focus measure EOG failed to satisfy the monotonicity requirement of focus metrics. And also, most of focus measures did not show a peak at the in-focus position, therefore they lack the capability of finding the in-focus position. Only

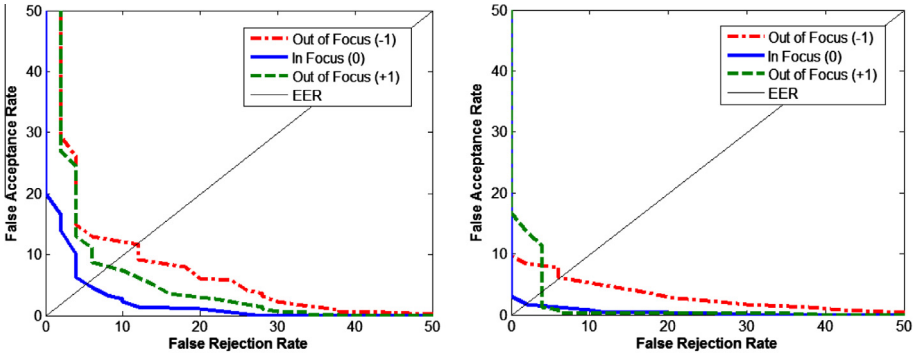

Fig. 3. ROC curves for each focusing position: (a) PCA and (b) LDA.

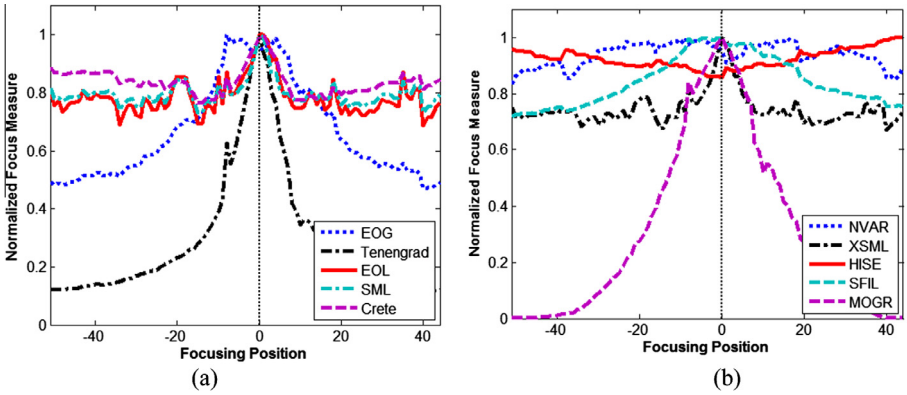

Fig. 4. Performance comparisons of 10 different focus measures.

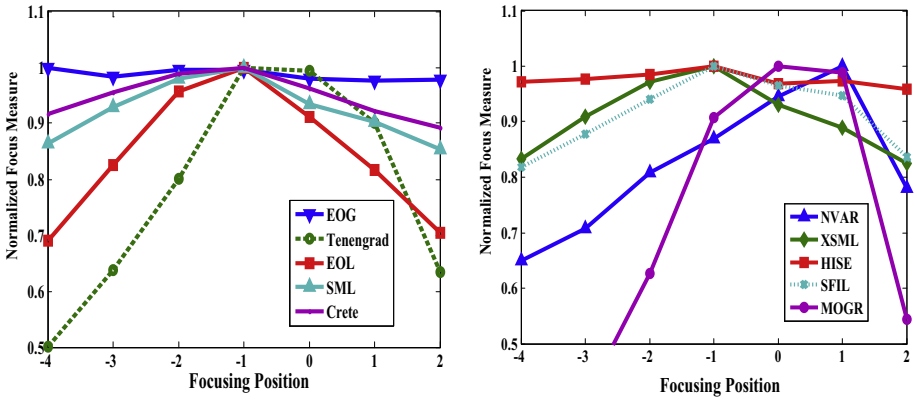

Fig. 5. Performance comparisons of 10 different focus measures.

Table 2
Summary of performances of 10 focus measures.

Focus measures	EOG	Tenengrad	EOL	SML	Crete	NVAR	XSML	HISE	SFIL	MOGR
In-focus (offset)	−4	−1	−1	−1	−1	+1	−1	−1	−1	0
Average ARM (step)	3.58	1.66	1.77	1.91	1.94	2.44	1.89	1.98	1.89	1.34
Monotonicity	N	Y	Y	Y	Y	Y	Y	Y	Y	Y
Average computation time (ms/image)	0.58	1.12	0.80	0.81	1.52	0.23	1.61	0.23	8.94	3.11

MOGR could successfully find the in-focus position. In Table 2, MOGR operator showed the lowest ARM steps of 1.34 on average. Therefore, MOGR is most preferred for thermal face recognition since the focus measure shows a large variation in terms of focus measure as well as zero offset. All the experiments were conducted on a computer with Intel Core i7 2.93 GHz processor, 4 GB RAM, Microsoft Windows 7 Professional K using a 32-bit MATLAB 7.13.0.564 (R2011b).

5. Conclusion

This paper evaluates the performance of widely used focus measures in terms of face recognition accuracies as well as sharpness in thermal IR imaging. Some focus measures, working properly for visible images, tend to underperform or even fail to find in-focus position in thermal IR imaging. Focusing quality significantly influences the performance of face recognition. The MOGR focus measure successfully finds in-focus position with highest face recognition accuracy and also satisfies the requirements of monotonicity and a large variation in focus measure along with low ARM with respect to the degree of blurring. Experiment results reveal that the nonlinear operations such as 'max' and 'min' used in the morphological gradient work better than the other focus measures for face recognition in thermal imaging, where intensity contrast is low and strong edge components of an object do not exist.

Acknowledgement

This research was supported by Basic Science Research Program through the National Research Foundation of Korea(NRF) funded by the Ministry of Education(2013R1A1A2011593).

References

Abate, A., Nappi, M., Riccio, D., Sabatino, G., 2007. 2D and 3D face recognition: a survey. Pattern Recognition Letters 28, 1885–1906.

Belhumeur, P., Hespanha, J., Kriegman, D., 1997. Eigenfaces vs. Fisherfaces: recognition using class specific linear projection. IEEE Transactions on Pattern Analysis and Machine Intelligence 19, 711–720.

Chen, X., Flynn, P., Bowyer, K., 2005. IR and visible light face recognition. Computer Vision and Image Understanding 99, 332–358.

Crete, F., Dolmiere, T., Ladret, P., Nicoras, M., 2007. The blur effect: perception and estimation with a new no-reference perceptual blur metric. In: SPIE Electronic Imaging Symposium on Human Vision and Electronic Imaging, 6492, pp. 64920I.1–64920I.11.

Faundez-Zanuy, M., Mekyska, J., Espinosa-Duro, V., 2011. On the focusing of thermal images. Pattern Recognition Letters 32, 1548–1557.

Gonzalez, R., Woods, R., 2010. Digital Image Processing, 3rd Edition. Pearson Prentice Hall, Upper Saddle River, New Jersey, USA.

Guo, L., Li, J., Li, Y., Wang, S., Jiang, A., 2008. Minimum image entropy technology applied to the real-time autofocusing system of space optical remote sensors. Proceedings of SPIE 7000, 700011.1–700011.7.

Huang, W., Jing, Z., 2007. Evaluation of focus measures in multi-focus image fusion. Pattern Recognition Letters 28, 493–500.

Kong, S., Heo, J., Abidi, B., Paik, J., Abidi, M., 2005. Recent advances in visual and infrared face recognition – a review. Computer Vision and Image Understanding 97, 103–135.

Minhas, R., Mohammed, A., Wu, Q., 2012. An efficient algorithm for focus measure computation in constant time. IEEE Transactions on Circuit and Systems for Video Technologies 22, 152–156.

Pertuz, S., Puig, D., Garcia, M.A., 2013. Analysis of focus measure operator for shape-from-focus. Pattern Recognition 46, 1415–1432.

Sang, J., Lei, Z., Li, S., 2009. Face image quality evaluation for ISO/IEC Standards 19794-5 and 29794-5, Lecture Notes in Computer Science, vol. 5558, pp. 229-238.

Santos, A., Solorzano, C., Vaquero, J., Pena, J., Malpica, N., Pozo, F., 1997. Evaluation of autofocus functions in molecular cytogenetic analysis. Journal of Microscopy 188, 264–272.

Subbarao, M., Tyan, J., 1998. Selecting the optimal measure for autofocusing and depth-from-focus. IEEE Transactions on Pattern Analysis and Machine Intelligence 20, 864–870.

Thelen, A., Frey, S., Hirsch, S., Hering, P., 2009. Improvements in shape-from-focus for holographic reconstruction with regard to focus operators, neighborhood-size, and height value interpolation. IEEE Transactions on Image Processing 18, 151–157.

Xie, H., Rong, W., Sun, L., 2006. Wavelet-based focus measure and 3-D surface reconstruction method for microscopy images. In: Proceedings of International Conference on Intelligent Robotics and Systems, pp. 229–234.